Building and Environment 167 (2020) 106424

Contents lists available at ScienceDirect

Building and Environment

journal homepage: http://www.elsevier.com/locate/buildenv

Classification and mapping of urban canyon geometry using Google Street View images and deep multitask learning

Chuan-Bo Hu [a,b], Fan Zhang [c,*], Fang-Ying Gong [d,e], Carlo Ratti [c], Xin Li [a]

[a] Lane Department of Computer Science and Electrical Engineering, West Virginia University, Morgantown, WV, 26505, USA
[b] Institute of Space and Earth Information Science, Chinese University of Hong Kong, Hong Kong, China
[c] Senseable City Laboratory, Massachusetts Institute of Technology, MA, 02139, USA
[d] School of Architecture, Chinese University of Hong Kong, Hong Kong, China
[e] California Institute of Technology, Pasadena, CA, USA

ARTICLE INFO

Keywords:
Street canyon classification
Built environment
Aspect ratio
Deep learning
Google Street View

ABSTRACT

Urban canyon classification plays an important role in analyzing the impact of urban canyon geometry on urban morphology and microclimates. Existing classification methods using aspect ratios require a large number of field surveys, which are often expensive and laborious. Moreover, it is difficult for these methods to handle the complex geometry of street canyons, which is often required by specific applications. To overcome these difficulties, we develop a street canyon classification approach using publicly available Google Street View (GSV) images. Our method is inspired by the latest advances in deep multitask learning based on densely connected convolutional networks (DenseNets) and tailored for multiple street canyon classification, i.e., H/W-based (Level 1), symmetry-based (Level 2), and complex-geometry-based (Level 3) classifications. We conducted a series of experiments to verify the proposed method. First, taking the Hong Kong area as an example, the method achieved an accuracy of 89.3%, 86.6%, and 86.1%, respectively for the three levels. Even using the field survey data as the ground truth, it gained approximately 80% for different levels. Then, we tested our pretrained model in five other cities and compared the results with traditional methods. The transferability and effectiveness of the scheme were demonstrated. Finally, to enrich the representation of more complicated street geometry, the approach can separately generate thematic maps of street canyons at multiple levels to better facilitate microclimatic studies in high-density built environments. The developed techniques for the classification and mapping of street canyons provide a cost-effective tool for studying the impact of complex and evolving urban canyon geometry on microclimate changes.

1. Introduction

With the acceleration of urbanization, the sustainable development of urban environments faces many challenges, such as the urban heat island effect [1], air quality deterioration [2], and urban greenway design [3]. Many of these challenges are closely related to prevailing high-rise, high-density residential and commercial development in downtown areas, which has made urban canyons, (also called street canyons), a growing concern over the past decade [4]. An example of a street canyon in the Hong Kong Island area is shown in Fig. 1. Researchers have paid increasing attention to the impact of high-density built environments on microclimate conditions, including the local temperature, wind conditions, and air quality [5]. Street canyon classification based on its geometric features has become an important basis for microclimate research in high-density areas.

Existing classification metrics of urban canyon geometry often depend on a range of factors such as the aspect ratio (AR) [6], the sky view factor [7] and the canyon orientation (e.g., north-south, east-west) [8]. Among them, the AR, which is the ratio of the canyon height (H) to the canyon width (W) $AR = H/W$, is an important factor for characterizing urban geometry. It has been used to classify street canyons into three basic categories (i.e., avenue canyons, regular canyons, and deep canyons) [9,10]. It was claimed in Ref. [6] that the generation of extreme thermal stress is closely related to various values of H/W. Different wind flow regimes in street canyons were defined in Ref. [11] based on H/W; in the increasing order of H/W, the roughness flow, wake

* Corresponding author.
E-mail address: zhangfan@mit.edu (F. Zhang).

https://doi.org/10.1016/j.buildenv.2019.106424
Received 17 May 2019; Received in revised form 21 September 2019; Accepted 23 September 2019
Available online 3 October 2019

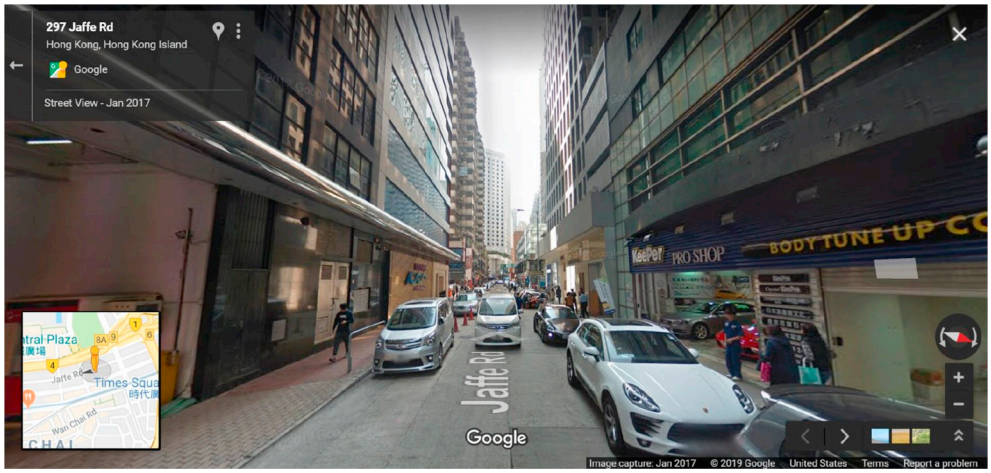

Fig. 1. An example of street canyon in the Hong Kong Island area. (Source: Google Maps, 2017).

interference flow and skimming flow were isolated.

Another classification metric of street canyons is based on the symmetry of street canyons, i.e., whether the heights of buildings on both sides of the street are similar. It was proposed in Ref. [12] that street canyon symmetry has an important influence on thermal comfort in urban street canyons. More recently, the effect of asymmetrical street H/W on microclimates in hot, humid regions was studied in Ref. [13]. They claimed that asymmetric streets are better than low symmetric streets in terms of enhancing the wind flow and blocking solar radiation, especially when tall buildings confront the wind's direction or solar altitudes. In addition, more complex street canyons (e.g., intersections, viaduct bridges and acoustic barriers) can be classified according to the practical needs in various applications [14–16].

However, most existing classifications heavily rely on a large amount of field survey data, including buildings, roads and other infrastructure data, which is time consuming, labor intensive and costly. Moreover, it makes the rapid update of data difficult. In addition, these data are often not publicly available, which restricts research on the impact of street canyon geometry on the environment. With rapid advances in sensing and computing technologies, we have access to large, publicly available data and unprecedented computational resources. For example, Google Street View (GSV) images have been widely used in quantitative research of built-environment and urban landscapes. GSV images cover 39 countries and approximately 3000 cities. This data source can be easily accessed by users with the Google map API [17]. In addition, GSV images can be updated frequently. More importantly, they contain detailed and actual information on urban landscapes, including the sky, trees, buildings and roads, which is valuable for urban canyon classification.

Recent rapid advances in deep learning have further stimulated interest in GSV image content analysis. The excellent performance of deep learning in many vision tasks, such as object recognition and image classification, has inspired a wide range of novel applications in other relevant domains, including geoscience and environmental engineering [18]. For instance, in Ref. [19], the authors demonstrated the feasibility of measuring sky, tree, and building view factors of street canyons based on deep learning and GSV images. In summary, this method demonstrates great promise by leveraging the latest advances in deep learning to more effectively extract useful information from GSV images and potentially support urban canyon analysis and classification tasks.

The aim of this study is to develop a GSV- and deep learning-based approach for street canyon classification and mapping in urban environments. A classification hierarchy for street canyons is proposed in terms of three levels: H/W-based, symmetry-based and complex-geometry-based classification. Furthermore, a deep multitask learning model for street canyon classification (DMLM-SCC) was designed based on the proposed multitask model. In the experiment, we take the Hong Kong area as an example to demonstrate the effectiveness and transferability of the proposed DMLM-SCC model by comparing it with traditional methods. Furthermore, an additional experiment for five other cities was presented for validation. The results show that the proposed DMLM-SCC model is suitable for street canyon classification and can potentially be used in the study of the impact of complex and evolving urban canyon geometry on microclimate changes.

2. Method

In this section, we present the proposed DMLM-SCC scheme. We first introduce GSV image collection process. Then, a classification hierarchy for refining the classification of street canyons based on their geometrical features from three levels is described. Finally, we present the multitask deep learning network for street canyon types prediction based on classification hierarchy.

2.1. GSV data collection

To construct a collection of classification maps with more variety of street canyon categories, we obtain the geospatial street vector data for a city from OpenStreetMap [20]. Point data with GPS coordinates are then generated by equally sampling the street vector data based on GIS software (e.g., ArcGIS). Finally, GSV images can be accessed and retrieved at each point location via the Google Map API, as the following example shows: https://maps.googleapis.com/maps/api/streetview/metadata?size=400x400&location=LAT,LON&heading=HEADING&fov=FOV&pitch=PITCH&key=APIKey. where LAT and LON are the latitude and longitude respectively, FOV determines the horizontal field of view of the image, HEADING is to indicate the compass heading of the camera, PITCH specifies whether the upper and lower angle of the camera is relative to the street view vehicle, and the API Key verification request is the required credentials.

This paper uses four street view images (i.e., $heading = 0, 90, 180, 270$) with $FOV = 120$ and $Pitch = 0$ from each point. This is because the four images are able to describe most of the information for street canyons in the scene.

2.2. Classification hierarchy for street canyon

This paper is devoted to the integration of existing street canyon classification metrics and proposes a classification method based on GSV images to refine the classification of street canyons. To achieve this goal, we designed a classification hierarchy for street canyons consisting of three levels, namely H/W-based (Level 1), symmetry-based (Level 2),

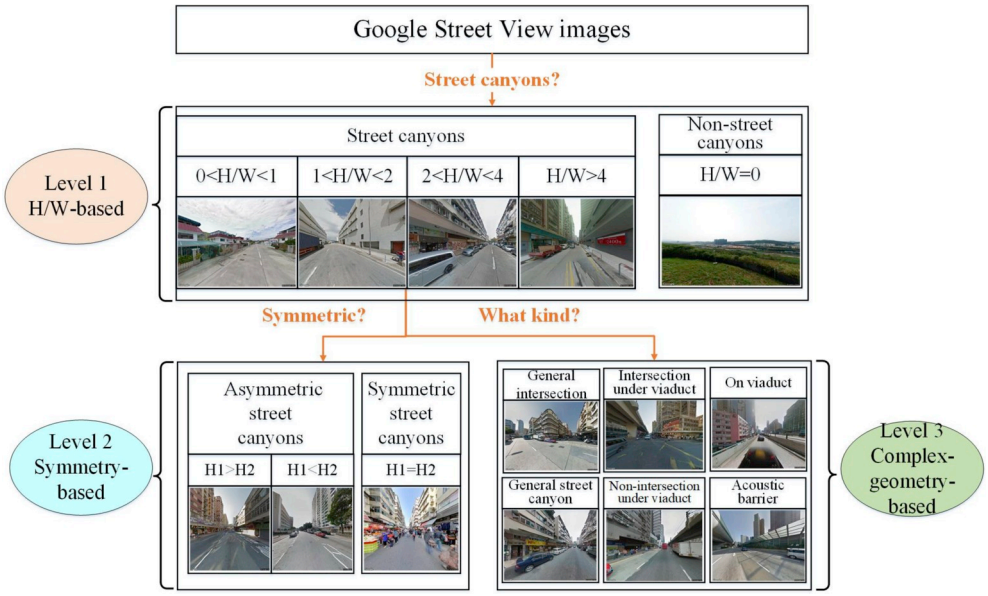

Fig. 2. A classification hierarchy for street canyon (note that traditional H/W-based approach is incorporated into Level 1 in our architecture).

- Level 1: Street canyons are classified based on their H/W value at Level 1. They are divided into non-street canyons and street canyons. The former is mainly some of the GSV images taken in parks, at the seaside and in the suburbs. The latter mainly divides street canyons into four categories according to H/W (i.e., $0 < H/W < 1$, $1 < H/W < 2$, $2 < H/W < 4$, and $H/W > 4$). If a street canyon decision is reached at Level 1, the architecture continues to perform classification tasks at Level 2 and Level 3.
- Level 2: Street canyons are classified based on their symmetry at Level 2. They are mainly divided into asymmetric street canyons and symmetric street canyons, which depends on whether the height of the buildings on both sides of the street are similar. Asymmetric street canyons are represented by $H_1 > H_2$ and $H_1 < H_2$. Symmetric street canyons are represented by $H_1 = H_2$, where H_1 is the height of the building on the left side of the street and H_2 is the height of the building on the right. The symmetry of street canyons has different effects on the thermal comfort, airflow and pollutant dispersion in different street orientations, including an $N-S$ orientation and an $E-W$ orientation [21–23].
- Level 3: Street canyons can also be categorized into a series of complex geometry features for specific application needs at Level 3. In this work, we focus on dividing these street canyons into intersections, viaducts (above and below), and acoustic barriers according to a large number of street canyon applications and based on complex geometry. This level is not limited to the six types of street canyons.

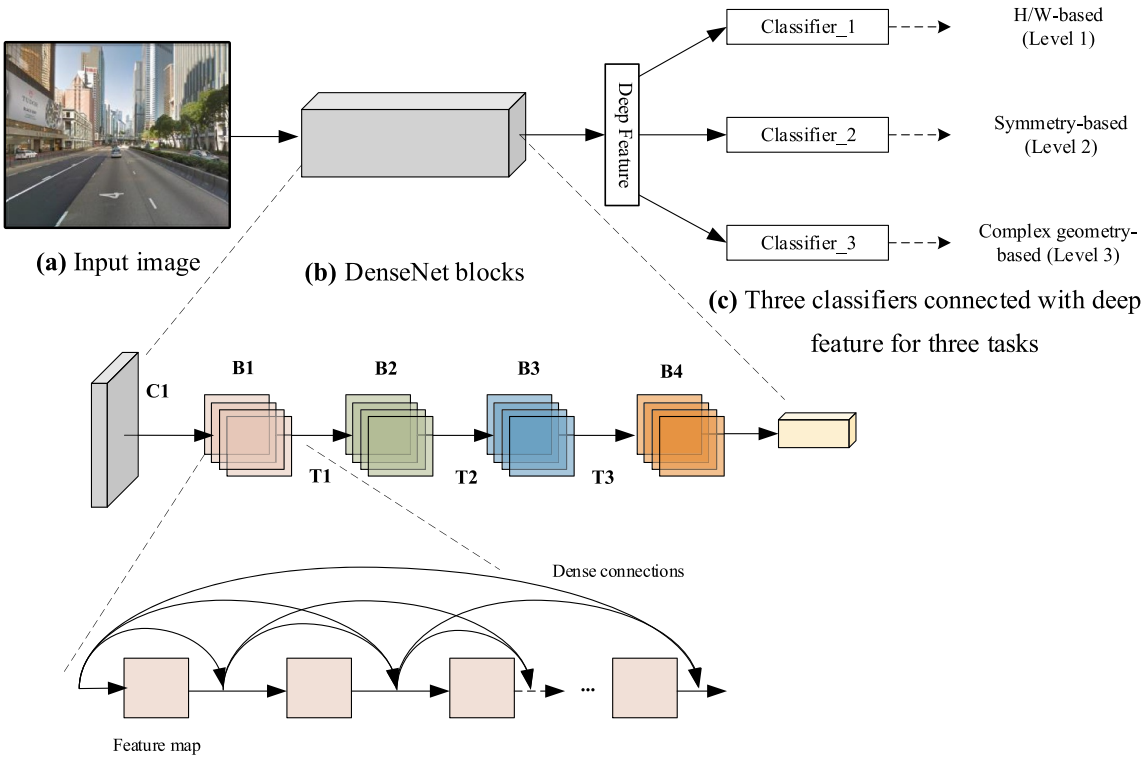

Fig. 3. The architecture of the proposed DCNN.

Table 1
Model architecture for street canyon classifications.

Name	Layers	#of Feature Maps	Filters	Output Size
Image	Input	3	None	224 × 224
C1	Convolution	64	conv(7 × 7)	56 × 56
	Pooling	64	avgpool(2 × 2)	56 × 56
B1	Dense Block	256	$\begin{bmatrix} conv(1\times1) \\ conv(3\times3) \end{bmatrix} \times 6$	56 × 56
T1	Convolution	128	conv(1 × 1)	56 × 56
	Pooling		avgpool(2 × 2)	28 × 28
B2	Dense Block	512	$\begin{bmatrix} conv(1\times1) \\ conv(3\times3) \end{bmatrix} \times 12$	28 × 28
T2	Convolution	256	conv(1 × 1)	28 × 28
	Pooling		avgpool(2 × 2)	14 × 14
B3	Dense Block	1024	$\begin{bmatrix} conv(1\times1) \\ conv(3\times3) \end{bmatrix} \times 24$	14 × 14
T3	Convolution	512	conv(1 × 1)	14 × 14
	Pooling		avgpool(2 × 2)	7 × 7
B4	Dense Block	1024	$\begin{bmatrix} conv(1\times1) \\ conv(3\times3) \end{bmatrix} \times 16$	7 × 7
Classification	Pooling	1024	avgpool(7 × 7)	1 × 1
	Ratio Classifer		softmax(1000, 5)	1
	Symmetry Classifer		softmax(1000, 3)	1
	Complex Classifer		softmax(1000, 6)	1

and complex-geometry-based (Level 3) classifications, as shown in Fig. 2.

2.3. DMLM-SCC scheme

Recently, deep learning-based models have been applied to a variety of computer vision tasks and have achieved great success in many applications such as image classification [24,25], image attribute prediction [26,27], image scene segmentation [28,29] and helping researchers understand places and cities [30,31]. Deep convolutional neural networks (DCNNs), which take inspiration from the neural structure of human brains, can automatically learn efficient features and conduct various visual inference tasks [32–34]. DCNN-based models have been designed to solve a wide range of both low-level (e.g., image restoration [35], image super-resolution [36] and image synthesis [37]) and high-level (e.g., visual concepts [38], context relations [28], and visual depth [39]) vision tasks.

Inspired by these works, we designed a deep convolutional neural network (DCNN) to classify street canyon geometry. We demonstrate that the proposed DMLM-SCC model is able to infer the street canyon geometry from three different aspects (see the previous section). Similar to the image scene understanding task, our learning-based approach

Table 2
Classification accuracy of DMLM-SCC based on GSV images.

Level	Overall Accuracy	Type	#of Test samples	Accuracy
Level 1	89.3%	Not a street canyon	1810	88.8%
		$0 < H/W < 1$	1465	86.5%
		$1 < H/W < 2$	3106	93.5%
		$2 < H/W < 4$	795	62.6%
		$H/W > 4$	2374	94.7%
Level 2	86.6%	$H_1 = H_2$	1781	78.4%
		$H_1 > H_2$	2566	87.7%
		$H_1 < H_2$	2540	91.3%
Level 3	86.1%	Intersection	1789	87.8%
		On a viaduct	2181	93.9%
		Intersection under a viaduct	611	75.9%
		Non-intersection under a viaduct	2942	89.6%
		Acoustic barrier	562	80.2%
		General street canyons	665	55.0%

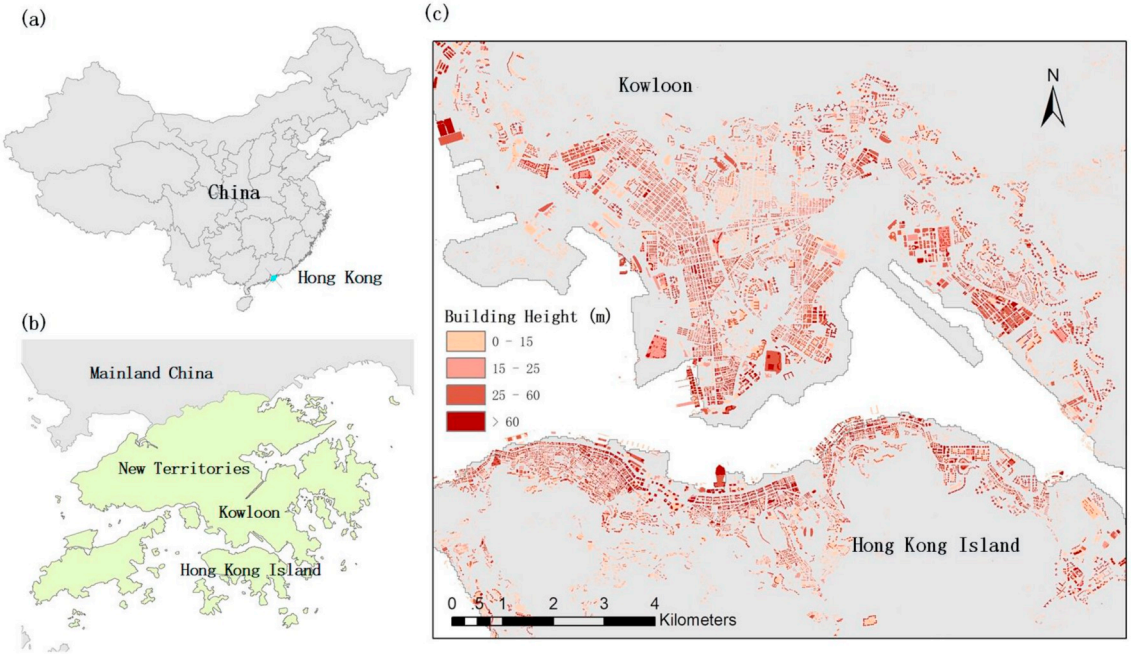

Fig. 4. The study area: Hong Kong, China; (a)Location of Hong Kong (blue points) in south-eastern China; (b) urban areas in Hong Kong; (c) High-density building environment in Kowloon and Hong Kong Island. (For interpretation of the references to color in this figure legend, the reader is referred to the Web version of this article.)

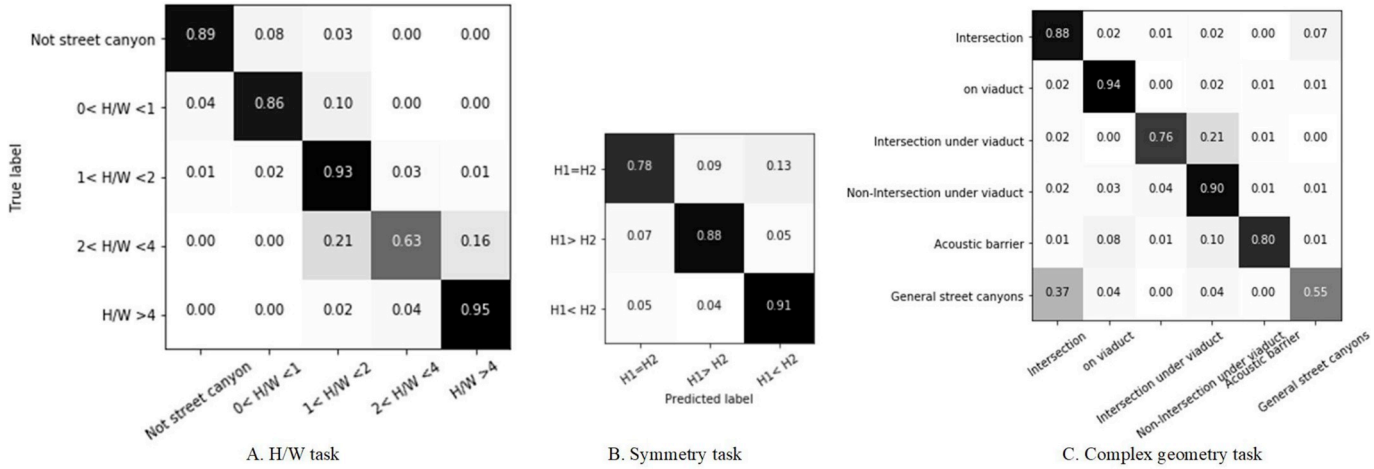

Fig. 5. Confusion matrices for the three classification tasks: (a) the H/W-based task, (b) the Symmetry-based task and (c) the complex-geometry-based task.

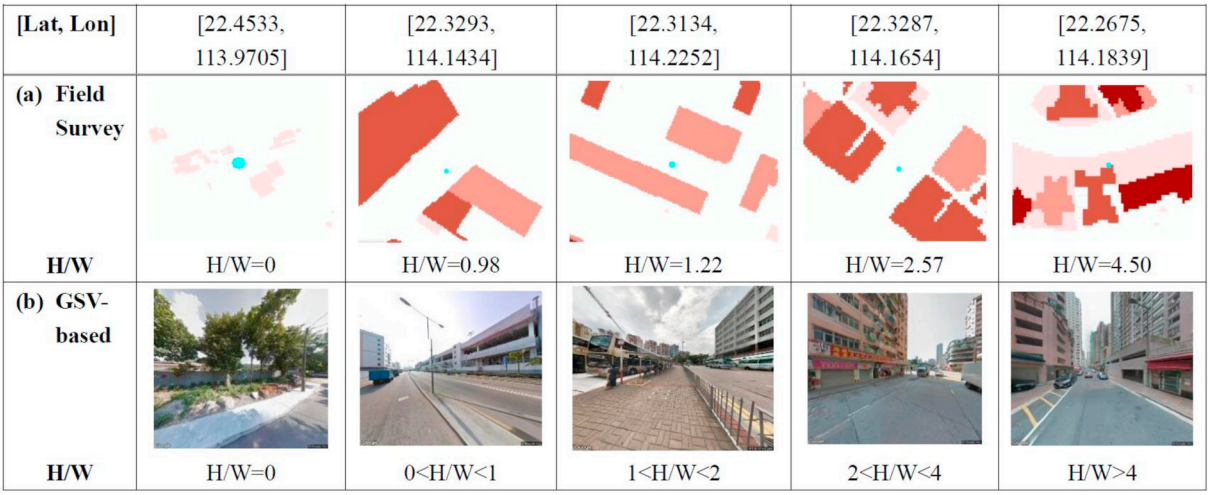

Fig. 6. Comparison of the H/W-based classification results with the field survey data.

- First, we randomly selected 100 points in Hong Kong and 100 points in Kowloon and Hong Kong Island with extremely high-density built environments. The former is to validate the classification results at Level 1, as shown in Fig. 6. The latter is to focus on the high-density built environment to validate the classification results at Level 2, as shown in Fig. 7.

does not require measuring building height and street width data with field surveys. Instead, the proposed DCNN will automatically learn the deep features to support the classification tasks. Conceptually similar to facial image classification (i.e., we can classify an image into different by gender, race and facial expression) [40], we have developed a multitask learning network to learn the shared deep feature representations among the three street canyon geometry classification tasks.

Our designed model is inspired by a recently developed DenseNet architecture [41] and multitask learning for face images [42]. DenseNet (densely connected convolutional networks) is a type of deep convolutional neural network. It concatenates outputs from all the previous layers to encourage feature reuse and to strengthen feature propagation. The DenseNet-based model has yielded outstanding performance in various computer vision tasks, such as object classification and scene understanding tasks [41,43].

Fig. 3 illustrates the architecture of the proposed model. For a 224× 224 input GSV image, a DenseNet-based network is employed to extract deep representations of the street scene. Compared with previous DCNNs, the largest improvement from DenseNet is its dense block architecture, where direct connections are introduced from any layer to all subsequent layers to improve the information flow between layers. Following the last convolution layer of DenseNet, three fully connected layers and softmax functions are designed for the three street canyon classification tasks. To implement the multitask training process, the loss for the "aspect ratio" task, the "symmetry" task and the "complexity" task is defined as $\mathscr{L}_{ratio}(w)$, $\mathscr{L}_{symmetry}(w)$ and $\mathscr{L}_{complexity}(w)$, respectively. We use cross-entropy loss for $L(\cdot)$. The training target is defined as follows:

$$\min_{w}\left\{\sum \mathscr{L}_{ratio}(w)+\mathscr{L}_{symmetry}(w)+\mathscr{L}_{complexity}(w)\right\} \quad (1)$$

The detailed network configuration is specified in Table 1. The network is mainly composed of four dense blocks (B1–B4). In each block, the feature maps from the last layer are processed by a composite function of operations including a certain number of 1×1 and 3×3 convolutional filters. As the input image passes through the whole network, the number of feature maps increases (from 2 to 1024) to extract the scene information from different perspectives. At the same time, the output size of the feature maps decreases (from 224×224 to 1×1) to reduce the amount of redundant information and keep the efficient features.

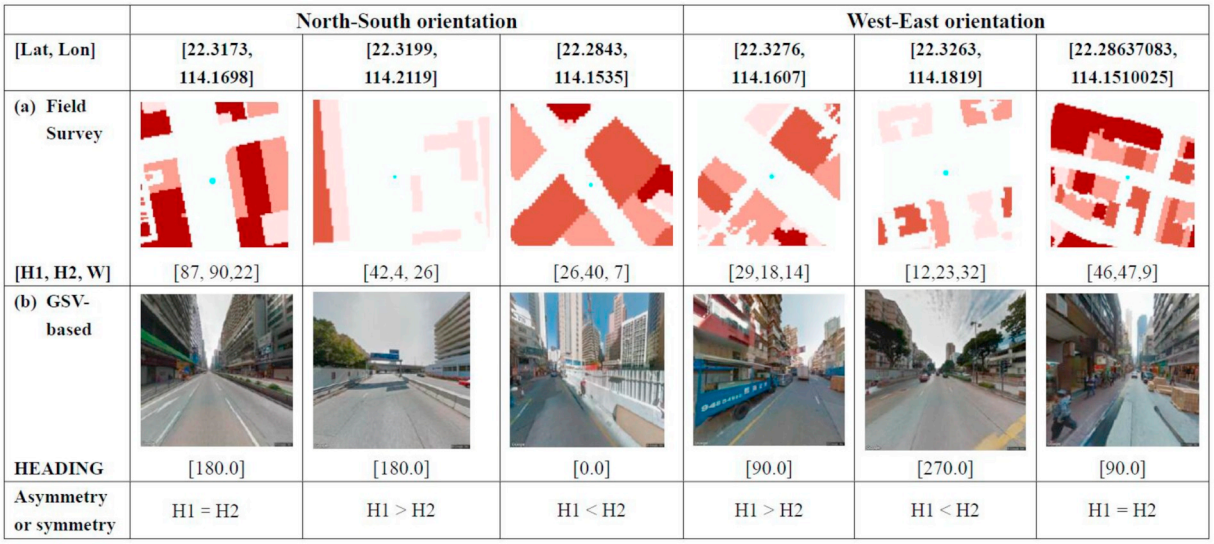

Fig. 7. Comparison of the symmetry-based classification results with the field survey data.

- Second, we labeled the height of the buildings on both sides of the street (H_1, H_2) and the width of the street section (W) for the 200 random sampled points. We first analyzed the images according to the HEADING of the image request, which is the compass heading of the camera. The classification results can be converted into specific street directions H_1 and H_2 by the heading of the image. Then, we calculated H_1/W, H_2/W and H/W (which is equal to the mean of H_1/W and H_2/W) based on the street orientations (i.e., $E-W$ and $N-S$) via the traditional H/W calculation method and compare the calculated results with the predicted results. If the predicted results from the trained DMLM-SCC model are consistent with the calculated results based on the field survey data, it is considered a correct classification; otherwise, it is considered an incorrect classification. Complex geometry calculation is only verified based on visual interpretation for images (see in Section 3.3.1) due to the lack of field survey data.

(1) Validation of the H/W-based classification task

Table 3
Classification accuracy for the 100 sampled points.

Level	Accuracy	Type	Number of samples	Subclass accuracy
Level 1	81.0%	Non-street canyon	25	96.0%
		$0 < H/W < 1$	15	93.3%
		$1 < H/W < 2$	42	71.4%
		$2 < H/W < 4$	6	66.7%
		$H/W > 4$	12	75.0%

3. Experiment

We take Hong Kong as the study area and implement the proposed method. Furthermore, we compared the proposed method and traditional street canyon classification method from a series of aspects. As an application, we mapped the different street canyon distributions of Hong Kong.

3.1. Study area

Hong Kong is one of the world's most densely populated cities with the highest building density. The high-density urban areas are characterized by high-rise compact building blocks and deep street canyons, as shown in Fig. 4. In these areas, it is common to see tall buildings over 40 stories located on narrow streets approximately 20 m wide. These complex street canyon environments are closely associated with serious problems, such as urban heat island effects, air pollution, radio reception issue, and human thermal discomfort. Therefore, how to classify and map street canyons becomes an important foundation for research on the built environment.

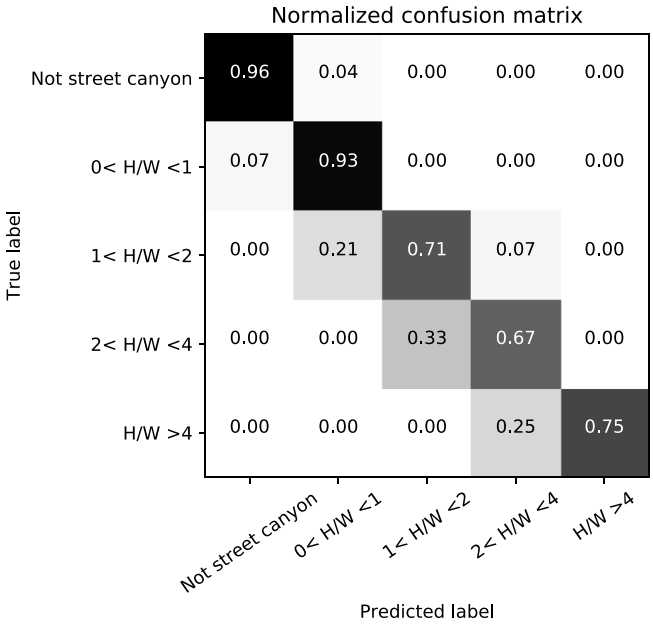

Fig. 8. Normalized confusion matrix of the 100 sampling points.

3.2. Experimental setup

To obtain a large amount of experimental data, we first used GIS software to generate the sampling locations from the OpenStreetMap along the streets of Hong Kong. Totally 109,118 sampling points (which can be used to obtain 436,472 GSV images) were collected in the study area. Then, we randomly selected 84,024 images to train the proposed DMLM-SCC model. These images were labeled by a third party and took approximately 40 h.

We divided these images into a training subset (70%) and a testing

Fig. 9. Symmetry-based classification result histogram.

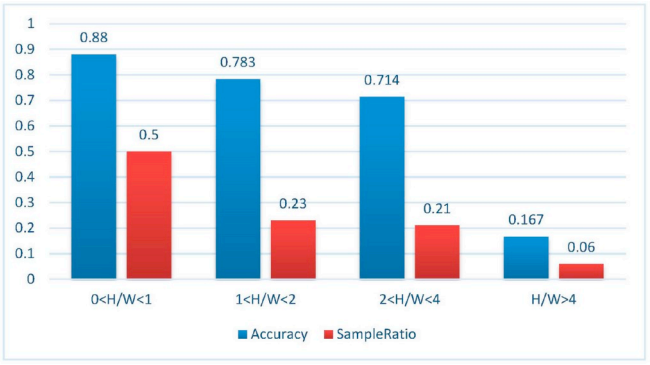

Fig. 10. Comparative analysis histogram based on H/W for the symmetry-based classification.

subset (30%) to ensure that there was no overlap between them. Using a workstation with an 8-core CPU and two NVIDIA 1080Ti GPUs (12G RAM) as the experimental environment, the designed DMLM-SCC took approximately 5 h to complete the training process. The trained model was tested on the testing subset. In addition, the model was evaluated on 200 randomly sampled points with ground truth data collected from field survey. Finally, all 436,472 images were predicted by the well-trained model. Accordingly, a street canyon distribution mapping can be drawn.

3.3. Experimental results

3.3.1. Classification accuracy of the DMLM-SCC model

The classification results of the DMLM-SCC model based on GSV images are shown in Table 2. If the predicted result of a GSV image from the trained DMLM-SCC model is consistent with the labeled type, it is regarded as a correct classification; otherwise, it is considered an incorrect classification. The Accuracy is determined based on the percentage of correct classifications. The model achieved an overall accuracy of 85% for the classification at the three levels. However, the $2 < H/W < 4$ subcategory at Level 1 achieved a low accuracy of 62.6% because of its small number of sample images. In addition, the general street canyon subcategory at Level 3 achieved the lowest, but still acceptable, accuracy due to the sample's diversity and complexity.

Fig. 5 presents the confusion matrices of the three tasks. The values in the matrix indicate the percentage that samples from one category were classified correctly into another category by the model. Generally, the confusion matrix presents how similar a pair of categories is according to the model's performance. We noted that some categories are misclassified into each other more easily because these categories are naturally and visually similar to each other, such as subcategories $1 < H/W < 2$ and $2 < H/W < 4$, with is reasonable.

3.3.2. Validation based on GIS field survey data

We used the following two steps to further validate the proposed method based on the field survey data of building and streets, which was extracted from the "B5000 maps series" by the Hong Kong Lands Department at Level 1 and Level 2.

The accuracy of the H/W-based classification results is 81% at Level 1, as shown in Table 3. Most sub-categories achieved an accuracy greater than 70%, except for the $2 < H/W < 4$ type. We further show the results based on the normalized confusion matrix of 100 sampled points in Fig. 8.

We noted that some categories were more susceptible to misclassification, such as the subcategories $1 < H/W < 2$ and $2 < H/W < 4$ as shown in Fig. 8. These results are similar to those in Fig. 5 (a) and show that the trained DMLM-SCC model achieves consistent results with the verification results based on the field survey data.

(2) Validation of the symmetry-based classification task

The overall accuracy of the symmetry-based classification results is 78% at Level 2. The comparison results of the street canyon classification in these two orientations are shown in Fig. 9. For each category, the

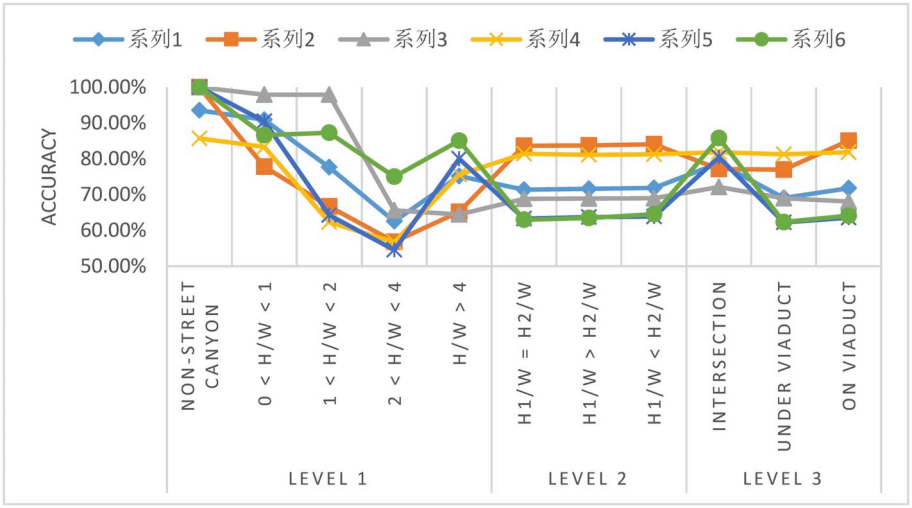

Fig. 11. Transferability to other cities.

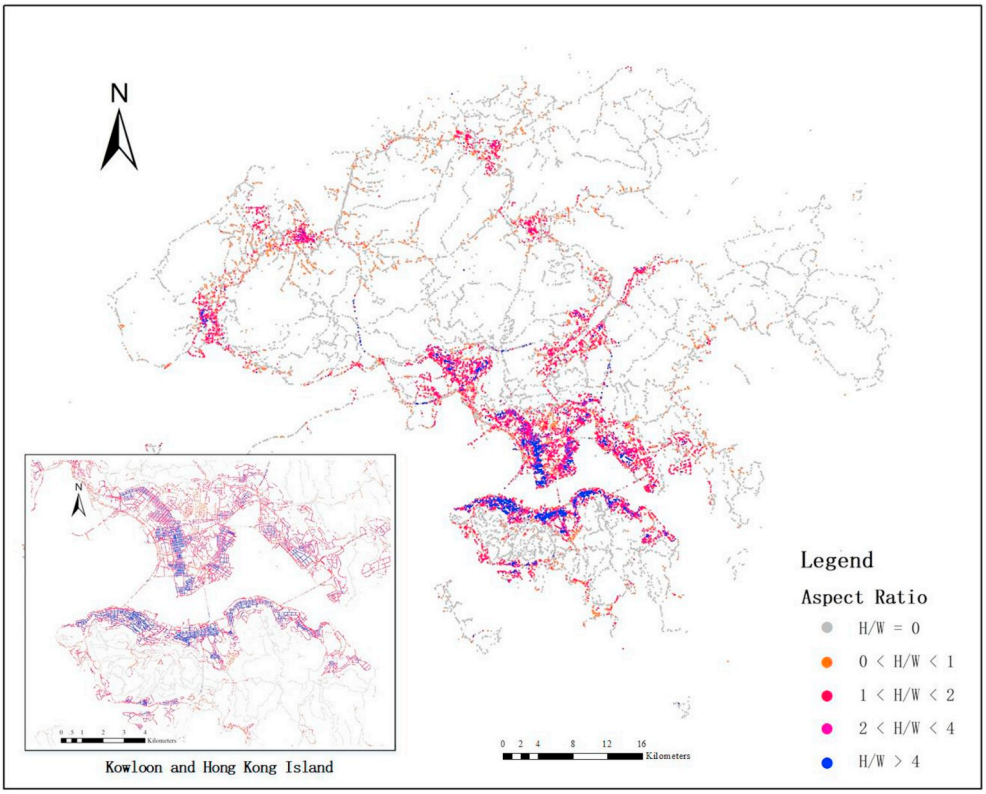

Fig. 12. The classification map of Hong Kong street canyons based on H/W (Level-1).

accuracy rates in the $E-W$ orientation are all lower than those in the $N-S$ orientation. This finding is attributed to the fact that the GSV images in the $E-W$ orientation are more susceptible to sunlight interference due to sunrise and sunset. These results will be further verified in Section 3.3.5.

To show the classification results based on symmetry more specifically, we give the overall accuracy rates in different H/W ranges in Fig. 10. We can observe that a higher accuracy (greater than over 70%) was achieved for the $0 < H/W < 1$, $1 < H/W < 2$ and $2 < H/W < 4$ categories, while the $H/W > 4$ category only gained 16.7% accuracy. This finding is due to the limited horizontal field of view of the GSV images. It is difficult to compare the height of buildings on both sides of the street in such extremely deep street canyons.

3.3.3. Transferability to other cities

To show the robustness and transferability of our proposed scheme, we tested the trained DMLM-SCC model in five other cities: London, Paris, Tokyo, New York and Chicago. In total, 904 points (2653 images) from the five cities were randomly sampled to calculate the accuracy for further verification. These images were labeled manually based on the street canyon classification hierarchy at Level 1 and Level 2. Considering the geolocation and urban morphological characteristics, we merged the six complex classes into three classes (i.e., intersections, on a viaduct, under a viaduct) for the five cities. The results are shown in Fig. 11.

Fig. 11 shows the accuracy of the trained DMLM-SCC model at each level in these five cities. The accuracy of non-street canyons and street canyons with $0 < H/W < 1$ at Level 1 achieved a better performance. For Level 2, the accuracy for London and Tokyo is better than in other cities (we suspect this is because the urban morphology in those two cities is simpler). The accuracy of intersections in the five cities are approximate at Level 3. Such results are reasonable because intersections in a street canyon have a similar geometry in each city.

3.3.4. Mapping of the street canyon classification in Hong Kong

As an application of the proposed classification method, we mapped all the Hong Kong street canyons based on the classification results. In total, 109,118 sampling points (436,472 images) were predicted by the trained model for the three levels. Therefore, three classification maps of the street canyon distribution were produced based on these predicted images. The classification map for Level 1 is shown in Fig. 12.

As shown in Fig. 12, street canyons are mainly distributed in the core areas of different districts of Hong Kong. The orange points represent the shallow street canyons that are mainly distributed at the junction of the core area and the suburbs, and the gray points represent the non-street canyons, mostly distributed in suburbs and parks, while deep street canyons (blue points) are mostly located on Hong Kong Island and in Kowloon Tong.

Fig. 13 shows the mapping result of the street canyons in Hong Kong from symmetry-based classification (Level-2). Most street canyons are distributed in the downtown areas of Hong Kong Island and Kowloon Tong. Asymmetric street canyons are mainly distributed along the coastline and around irregular street layouts in high-density urban areas. Symmetrical street canyons are mainly distributed in the downtown core area with a regular street layout. Such a symmetry-based analysis will be useful for researching the thermal environment, wind environment and air quality because asymmetric street canyons have greater access to the sky [12,23].

Fig. 14 shows the mapping of different kinds of street canyons in Hong Kong. The most dense blue points are intersections in street canyons; gray points are non-street canyons that are predicted from Level 1. Points in other colors are related to the street environment of the viaduct, including the bridge, the space under the bridge and acoustic barriers. In fact, the Level 3 analysis is not limited to these types. It can be further extended to more detailed classifications tailored for specific application needs. It can be observed from Fig. 14 that there are a large number of intersections and viaducts in Hong Kong to divert traffic, especially in the street canyon. These observations help understand the

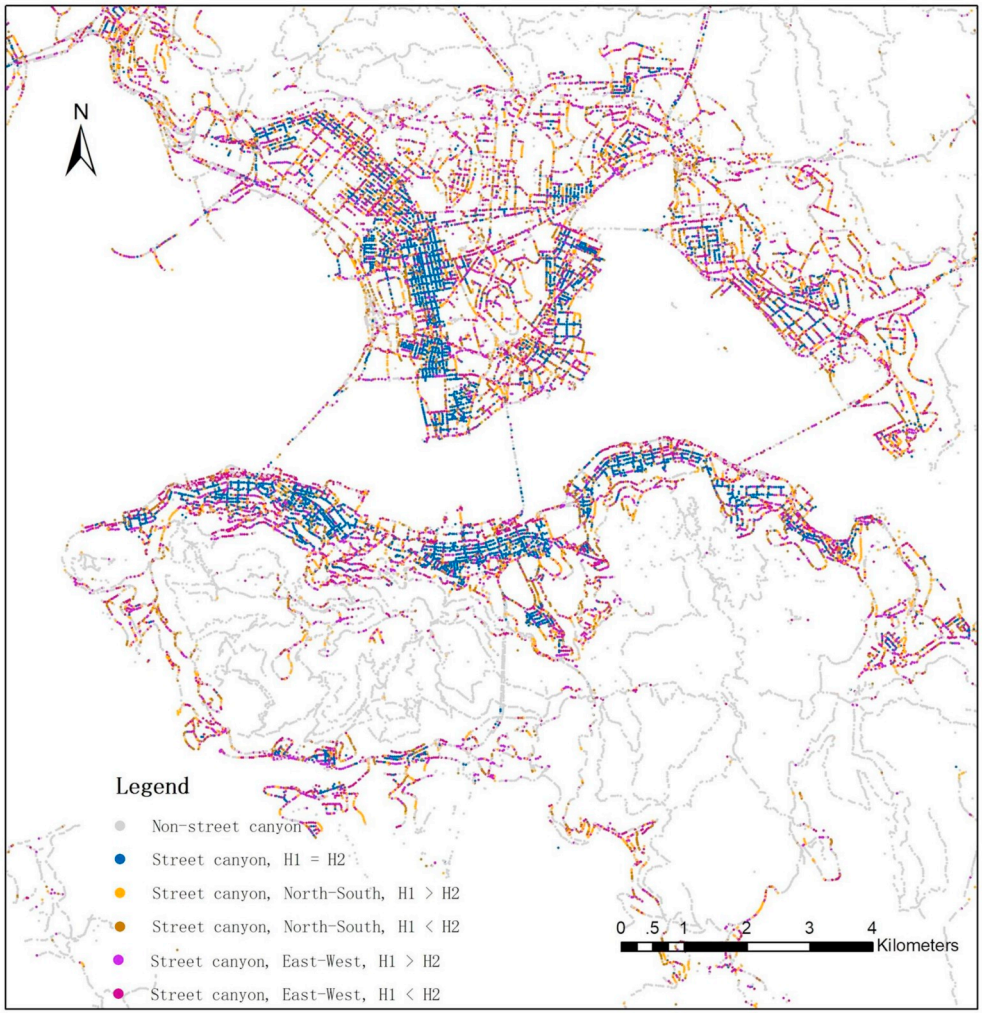

Fig. 13. The classification map of Hong Kong street canyons based on symmetry (Level-2).

road morphology and road type in the study area.

3.3.5. *Comparison DMLM-SCC with traditional street canyon classification*

Table 4 shows the comparison between the proposed method and traditional methods. The method from [9] has a high classification accuracy, medium calculation complexity but low transferability. In [10], two algorithms were developed to parameterize the urban morphology based on a traditional method. It defines a set of rules to generalize various street canyon calculation scenarios and is implemented as ArcPy Python tools within ArcGIS. It reduces the computational complexity while maintaining high accuracy. However, both algorithms require a large amount of field survey data including building geometry and street geometry.

In contrast, the proposed method can achieve medium accuracy (89.3%, 86.6% and 86.1% for three levels respectively) by using publicly available GSV images without relying on field survey data. This method can output different types of classifications and calibrations based on deep learning. As the number of classification categories increases, the computational complexity increases. In addition, we compared them in mapping applications with traditional methods as shown in Table 5.

The former two methods have lower update frequencies due to their dependence on field survey data. These methods require much manual labor and resources for high-frequency repeated measurements. In addition, they can only be used to map street canyons based on H/W and symmetry because of field survey data limitations. Mapping complex street canyons requires much complex data. However, the proposed method can update the map at a higher frequency because of the fast update of GSV images. Moreover, it can map street canyons into three layers (described in Section 3.4) because street view images can reflect a more elaborate street environment.

3.3.6. *Impact of sunshine on street canyon classification*

The sunlight in the open space of a street will have an impact on the quality of GSV images and thus affect the street classification results based on the proposed method. As shown in Fig. 15, the accuracy of street canyon classification in the $E-W$ orientation may be lower than that in the $N-S$ orientation. To verify this, we have selected the incorrectly classified GSV images from 100 sample points at Level 2 and divided the 100 sampled points into two categories: sunny (51 sampling points) and cloudy (49 sampling points). These two types are analyzed individually with their accuracy based on symmetry classification.

The results show that the accuracy of the sunny category is 76.5% while the accuracy of the cloud category is 100%. As the sun rises and sets, the GSV images in the $E-W$ orientation will sometimes be interfered with by more intense sunlight than those in the $N-S$ direction. This finding is basically consistent with the experimental results reported in Section 3.3.2.

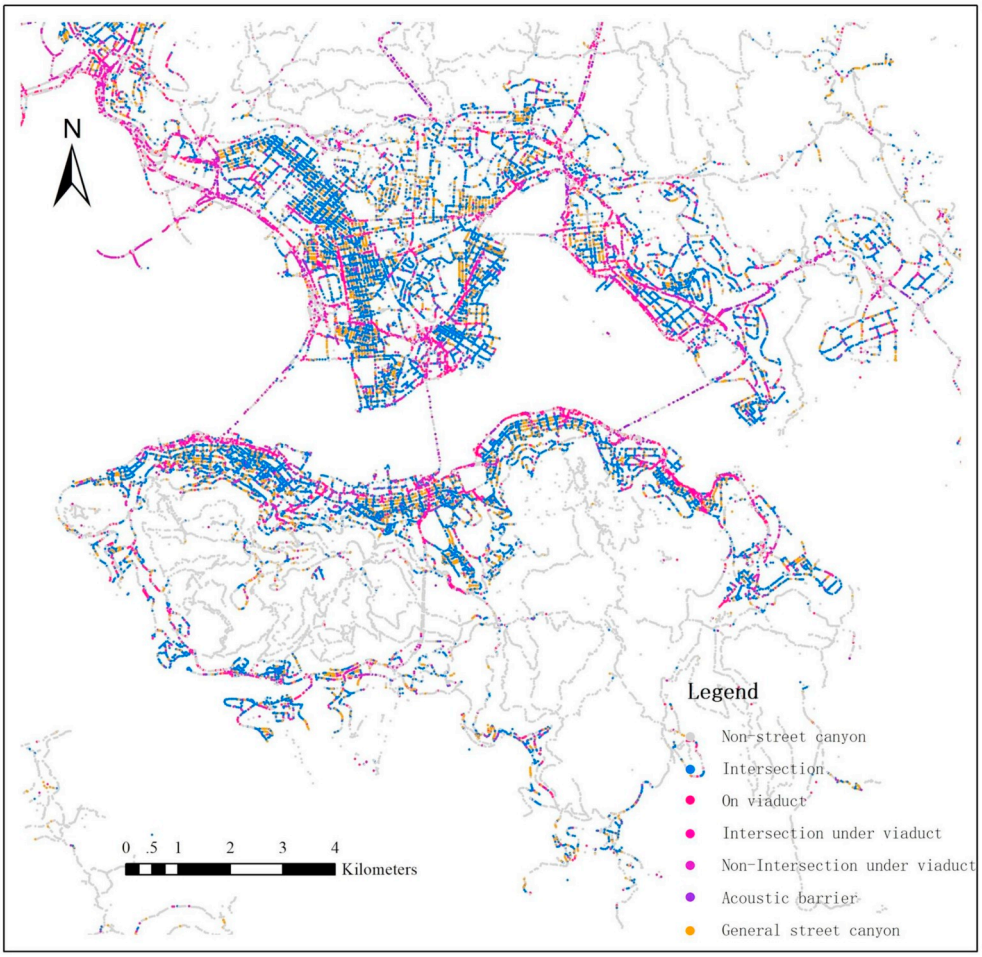

Fig. 14. The classification map of Hong Kong street canyons based on complex geometry (Level-3).

Table 4
Comparison of different methods for street canyon classification.

Criteria		Vardoulakis and Bernard [9]	Jackson and Hood [10]	Proposed
Accuracy		**High**	**High**	Medium
Calculation complexity		Medium	**Low**	High
Expansibility		Low	Low	**High**
Public available data				✓
Field survey data (GIS)	Building geometry	✓	✓	
	Road geometry	✓	✓	

Table 5
Comparison of the mapping properties from different classification methods.

Criteria		Vardoulakis and Bernard [9]	Jackson and Hood [10]	Proposed
Update Frequency		Low	Low	High
Multi-layer	Aspect Ratio-based layer	✓	✓	✓
	Symmetry-based layer	✓	✓	✓
	Complex street canyon layer			✓

4. Discussion and future work

4.1. Street view images offer a cost-effective solution for street canyon classification

We have shown that the proposed DMLM-SCC method can classify street canyons effectively from publicly available GSV images through a deep learning approach. Applying DMLM-SCC to study the urban geometry in Hong Kong, we found that the method yielded satisfactory classification results, as demonstrated in the validation phase based on field survey data. Compared with traditional methods, this study provides a cost-effective alternative solution to potentially support urban microclimate change research because it does not rely on expensive field survey data. Indeed, the proposed learning-based approach can have a higher refresh frequency than traditional methods because GSV images can be updated frequently. As a popular data source, street view imagery can be accessed from other open sources and crowdsourcing platforms, such as Mappillary. In addition, incorporated with Lidar data, street view images have become an important basis for the development of autonomous vehicles and City Information Model, which makes this data sources easier to access. Besides, it is expected that the proposed approach can help explore the correlation between street canyons and microclimates, especially in developing countries, to better support their urbanization processes.

Fig. 15. Misclassified GSV images are affected by sunlight.

4.2. Refined classification maps of street canyons support evidence-based interdisciplinary research on urban issues

In this paper, we show that the proposed DMLM-SCC model outperforms the existing methods in terms of the following: (1) it can be extended to other cities without field survey data (see Section 3.3.3), and (2) it can be used to analyze how different types of street canyons at multiple levels affect local microclimate change in a more refined way, because this method can classify street canyons more efficiently. In addition, according to previous works, the tree view factor, sky view factor and building view factor can be extracted from GSV panoramic images [19]. The incorporating of the proposed approach is promising for understanding the impact of green infrastructure, sky openness, and building density on microclimates in different types of street canyon environments.

4.3. Future work

In this work, we used natural street view imagery instead of hemispherical or panoramic images, which require accurate geometric and photogrammetric parameters to reconstruct the 3D environment. Nevertheless, the latter approaches have an advantage in understanding extremely deep street canyons. Therefore, in our future work, we will consider combining street view images with natural, hemispherical and panoramic view to improve the performance of street canyon classification. Furthermore, it is promising to use the local adaptive histogram equalization algorithm [44] to repair GSV images that are disturbed by sunlight. It can be achieved by first detecting the region affected by sunlight in a GSV image and then recovering the image based on the local adaptive histogram equalization algorithm. The above solution may be applicable to general GSV images affected by sunlight. Last but not least, it is expected that developing automatic tools for analyzing dynamic changes/differences from longitudinal GSV images, which is important in urban planning and development.

5. Conclusion

This study has focused on (1) developing a deep learning convolutional neural network for accurately classifying street canyons from multiple aspects using publicly available GSV images; (2) verifying the accuracy of the proposed GSV-based method by using construction and road reference data from a field survey; (3) comparing traditional methods with proposed methods and analyzing the influencing factors of the differences between them. A multi-layer classification map of street canyons (i.e., H/W-based, symmetry-based and complex-geometry-based) in Hong Kong was generated. The following conclusions can be drawn:

- The three-level street canyon classification accuracy values based on GSV images were 89.3%, 86.6% and 86.1%, respectively. This proves that the proposed method is a low-cost street classification method that does not rely on a large amount of field survey data.
- Verification with field survey data shows that the proposed method has a satisfactory accuracy and thus proves its effectiveness. The street canyon classifications based on symmetry are limited by high building densities and narrow street environments. In addition, they are limited by sunlight.
- This paper separately maps the street canyons from multiple levels, including the H/W-based, symmetry-based and complex-geometry-based. The detailed classification of street canyons from different levels can help meet the requirements of high-density urban microclimate environmental research.

Declaration of competing interest

The authors declare that there is no conflict of interest.

Acknowledgement

The funding support for this research is provided by the National Natural Science Foundation of China under Grant 41901321. Chuanbo Hu and Xin Li's work is partially supported by the DoJ/NIJ under grant NIJ 2018-75-CX-0032, NSF under grant OAC-1839909 and the WV Higher Education Policy Commission Grant (HEPC.dsr.18.5). The authors would also like to gratefully thank the members of the MIT Senseable City Lab Consortium: RATP, Dover Corporation, Teck Resources, Lab Campus, Anas S.p.A., Ford, SNCF Gares & Connexions, Brose, Allianz, ENEL Foundation, Laval, Curitiba, Stockholm, Amsterdam, Victoria State Government, KTH Royal Institute of Technology, UTEC - Universidad de Ingenier–a y Tecnología, Politecnico di Torino, Austrian Institute of Technology, Fraunhofer Institute, Kuwait-MIT Center for Natural Resources, SMART - Singapore-MIT Alliance for Research and Technology, and AMS Institute for supporting this research.

References

[1] T.R. Oke, The energetic basis of the urban heat island, Q. J. R. Meteorol. Soc. 108 (1982) 1–24.
[2] E. Krüger, F. Minella, F. Rasia, Impact of urban geometry on outdoor thermal comfort and air quality from field measurements in curitiba, Brazil, Build. Environ. 46 (2011) 621–634.
[3] P.H. Gobster, L.M. Westphal, The human dimensions of urban greenways: planning for recreation and related experiences, Landsc. Urban Plan. 68 (2004) 147–165.
[4] E. Alexandri, P. Jones, Temperature decreases in an urban canyon due to green walls and green roofs in diverse climates, Build. Environ. 43 (2008) 480–493.
[5] Y. Nakamura, T.R. Oke, Wind, temperature and stability conditions in an east-west oriented urban canyon, Atmos. Environ. 22 (1967) 2691–2700, 1988.

[6] F. Ali-Toudert, H. Mayer, Numerical study on the effects of aspect ratio and orientation of an urban street canyon on outdoor thermal comfort in hot and dry climate, Build. Environ. 41 (2006) 94–108.
[7] L. Zeng, J. Lu, W. Li, Y. Li, A fast approach for large-scale sky view factor estimation using street view images, Build. Environ. 135 (2018) 74–84.
[8] F.-Y. Gong, Z.-C. Zeng, E. Ng, L.K. Norford, Spatiotemporal patterns of street-level solar radiation estimated using google street view in a high-density urban environment, Build. Environ. 148 (2019) 547–566.
[9] S. Vardoulakis, B.E. Fisher, K. Pericleous, N. Gonzalez-Flesca, Modelling air quality in street canyons: a review, Atmos. Environ. 37 (2003) 155–182.
[10] M. Jackson, C. Hood, C. Johnson, K. Johnson, Calculation of urban morphology parameterisations for london for use with the adms-urban dispersion model, Int. J. Adv. Remote Sens. GIS 5 (2016) 1678–1687.
[11] T.R. Oke, Street design and urban canopy layer climate, Energy Build. 11 (1988) 103–113.
[12] F. Ali-Toudert, H. Mayer, Effects of asymmetry, galleries, overhanging facades and vegetation on thermal comfort in urban street canyons, Sol. Energy 81 (2007) 742–754.
[13] A. Qaid, D.R. Ossen, Effect of asymmetrical street aspect ratios on microclimates in hot, humid regions, Int. J. Biometeorol. 59 (2015) 657–677.
[14] J. Hang, Z. Luo, X. Wang, L. He, B. Wang, W. Zhu, The influence of street layouts and viaduct settings on daily carbon monoxide exposure and intake fraction in idealized urban canyons, Environ. Pollut. 220 (2017) 72–86.
[15] A. Wania, M. Bruse, N. Blond, C. Weber, Analysing the influence of different street vegetation on traffic-induced particle dispersion using microscale simulations, J. Environ. Manag. 94 (2012) 91–101.
[16] T. Van Renterghem, E. Salomons, D. Botteldooren, Parameter study of sound propagation between city canyons with a coupled fdtd-pe model, Appl. Acoust. 67 (2006) 487–510.
[17] X. Li, C. Zhang, W. Li, R. Ricard, Q. Meng, W. Zhang, Assessing street-level urban greenery using google street view and a modified green view index, Urban For. Urban Green. 14 (2015) 675–685.
[18] X. Li, C. Ratti, I. Seiferling, Quantifying the shade provision of street trees in urban landscape: a case study in boston, USA, using google street view, Landsc. Urban Plan. 169 (2018) 81–91.
[19] F.-Y. Gong, Z.-C. Zeng, F. Zhang, X. Li, E. Ng, L.K. Norford, Mapping sky, tree, and building view factors of street canyons in a high-density urban environment, Build. Environ. 134 (2018) 155–167.
[20] J. Kang, M. Körner, Y. Wang, H. Taubenböck, X.X. Zhu, Building instance classification using street view images, ISPRS J. Photogrammetry Remote Sens. 145 (2018) 44–59.
[21] J. Gallagher, L.W. Gill, A. McNabola, Numerical modelling of the passive control of air pollution in asymmetrical urban street canyons using refined mesh discretization schemes, Build. Environ. 56 (2012) 232–240.
[22] J.-J. Baik, R.-S. Park, H.-Y. Chun, J.-J. Kim, A laboratory model of urban street-canyon flows, J. Appl. Meteorol. 39 (2000) 1592–1600.
[23] I. Nikolova, S. Janssen, P. Vos, K. Vrancken, V. Mishra, P. Berghmans, Dispersion modelling of traffic induced ultrafine particles in a street canyon in antwerp, Belgium and comparison with observations, Sci. Total Environ. 412 (2011) 336–343.
[24] K. He, X. Zhang, S. Ren, J. Sun, Deep residual learning for image recognition, in: Proceedings of the IEEE Conference on Computer Vision and Pattern Recognition, pp. 770–778.
[25] G. Huang, Z. Liu, K. Q. Weinberger, L. van der Maaten, Densely connected convolutional networks, in: Proceedings of the IEEE Conference on Computer Vision and Pattern Recognition, pp. 2261–2269.
[26] B. Zhou, A. Lapedriza, A. Khosla, A. Oliva, A. Torralba, Places: A 10 Million Image Database for Scene Recognition, IEEE Transactions on Pattern Analysis and Machine Intelligence, 2017.
[27] F. Zhang, B. Zhou, L. Liu, Y. Liu, H.H. Fung, H. Lin, C. Ratti, Measuring human perceptions of a large-scale urban region using machine learning, Landsc. Urban Plan. 180 (2018) 148–160.
[28] B. Zhou, H. Zhao, X. Puig, S. Fidler, A. Barriuso, A. Torralba, Scene parsing through ade20k dataset, in: Proceedings of the IEEE Conference on Computer Vision and Pattern Recognition, pp. 5122–5130.
[29] F. Zhang, D. Zhang, Y. Liu, H. Lin, Representing place locales using scene elements, Comput. Environ. Urban Syst. 71 (2018) 153–164.
[30] M. Helbich, Y. Yao, Y. Liu, J. Zhang, P. Liu, R. Wang, Using deep learning to examine street view green and blue spaces and their associations with geriatric depression in beijing, China, Environ. Int. 126 (2019) 107–117.
[31] Y. Kang, Q. Jia, S. Gao, X. Zeng, Y. Wang, S. Angsuesser, Y. Liu, X. Ye, T. Fei, Extracting human emotions at different places based on facial expressions and spatial clustering analysis, Trans. GIS 23 (2019) 450–480.
[32] Y. LeCun, Y. Bengio, G. Hinton, Deep learning, Nature 521 (2015) 436–444.
[33] D. Hassabis, D. Kumaran, C. Summerfield, M. Botvinick, Neuroscience-inspired artificial intelligence, Neuron 95 (2017) 245–258.
[34] A. Banino, C. Barry, B. Uria, C. Blundell, T. Lillicrap, P. Mirowski, A. Pritzel, M. J. Chadwick, T. Degris, J. Modayil, et al., Vector-based navigation using grid-like representations in artificial agents, Nature 557 (2018) 429.
[35] K. Zhang, W. Zuo, Y. Chen, D. Meng, L. Zhang, Beyond a Gaussian denoiser: residual learning of deep cnn for image denoising, IEEE Trans. Image Process. 26 (2017) 3142–3155.
[36] C. Ledig, L. Theis, F. Huszár, J. Caballero, A. Cunningham, A. Acosta, A. Aitken, A. Tejani, J. Totz, Z. Wang, et al., Photo-realistic single image super-resolution using a generative adversarial network, in: Proceedings of the IEEE Conference on Computer Vision and Pattern Recognition, pp. 4681–4690.
[37] J.-Y. Zhu, T. Park, P. Isola, A. A. Efros, Unpaired image-to-image translation using cycle-consistent adversarial networks, in: Proceedings of the IEEE International Conference on Computer Vision, pp. 2223–2232.
[38] D. Bau, B. Zhou, A. Khosla, A. Oliva, A. Torralba, Network dissection: quantifying interpretability of deep visual representations, in: Proceedings of the IEEE Conference on Computer Vision and Pattern Recognition.
[39] L. He, G. Wang, Z. Hu, Learning depth from single images with deep neural network embedding focal length, IEEE Trans. Image Process. 27 (2018) 4676–4689.
[40] Z. Zhang, P. Luo, C. C. Loy, X. Tang, Facial landmark detection by deep multi-task learning, in: European Conference on Computer Vision, Springer, pp. 94–108.
[41] Y. Zhu, S. Newsam, Densenet for dense flow, in: IEEE International Conference on Image Processing, IEEE, pp. 790–794.
[42] R. Ranjan, V.M. Patel, R. Chellappa, Hyperface: a deep multi-task learning framework for face detection, landmark localization, pose estimation, and gender recognition, IEEE Trans. Pattern Anal. Mach. Intell. 41 (2019) 121–135.
[43] F. Zhang, L. Wu, D. Zhu, Y. Liu, Social sensing from street-level imagery: a case study in learning spatio-temporal urban mobility patterns, ISPRS J. Photogrammetry Remote Sens. 153 (2019) 48–58.
[44] K.M. Atanassov, J.W. Nash, S.M. Verrall, H.A. Siddiqui, Local adaptive histogram equalization, US Patent App 14/309 (2015) 458.